

ORIGINAL RESEARCH

High-Risk Plaques on Coronary Computed Tomography Angiography

Correlation With Optical Coherence Tomography



Daisuke Kinoshita, MD, PhD,^{a,*} Keishi Suzuki, MD, PhD,^{a,*} Eisuke Usui, MD, PhD,^b Masahiro Hada, MD, PhD,^b Haruhito Yuki, MD,^a Takayuki Niida, MD, PhD,^a Yoshiyasu Minami, MD, PhD,^c Hang Lee, PhD,^d Iris McNulty, RN,^a Junya Ako, MD, PhD,^c Maros Ferencik, MD, PhD, MCR,^e Tsunekazu Kakuta, MD, PhD,^b Ik-Kyung Jang, MD, PhD^{a,f}

ABSTRACT

BACKGROUND Although patients with high-risk plaque (HRP) on coronary computed tomography angiography (CTA) are reportedly at increased risk for future cardiovascular events, individual HRP features have not been systematically validated against high-resolution intravascular imaging.

OBJECTIVES The aim of this study was to correlate HRP features on CTA with plaque characteristics on optical coherence tomography (OCT).

METHODS Patients who underwent both CTA and OCT before coronary intervention were enrolled. Plaques in culprit vessels identified by CTA were evaluated with the use of OCT at the corresponding sites. HRP was defined as a plaque with at least 2 of the following 4 features: positive remodeling (PR), low-attenuation plaque (LAP), napkin-ring sign (NRS), and spotty calcification (SC). Patients were followed for up to 3 years.

RESULTS The study included 448 patients, with a median age of 67 years and of whom 357 (79.7%) were male, and 203 (45.3%) presented with acute coronary syndromes. A total of 1,075 lesions were analyzed. All 4 HRP features were associated with thin-cap fibroatheroma. PR was associated with all OCT features of plaque vulnerability, LAP was associated with lipid-rich plaque, macrophage, and cholesterol crystals, NRS was associated with cholesterol crystals, and SC was associated with microvessels. The cumulative incidence of the composite endpoint (target vessel nontarget lesion revascularization and cardiac death) was significantly higher in patients with HRP than in those without HRP (4.7% vs 0.5%; $P = 0.010$).

CONCLUSIONS All 4 HRP features on CTA were associated with features of vulnerability on OCT. (Massachusetts General Hospital and Tsuchiura Kyodo General Hospital Coronary Imaging Collaboration; [NCT04523194](#)) (J Am Coll Cardiol Img 2024;17:382–391) © 2024 by the American College of Cardiology Foundation.

From the ^aCardiology Division, Massachusetts General Hospital, Harvard Medical School, Boston, Massachusetts, USA; ^bDepartment of Cardiovascular Medicine, Tsuchiura Kyodo General Hospital, Tsuchiura, Ibaraki, Japan; ^cDepartment of Cardiovascular Medicine, Kitasato University School of Medicine, Sagami-hara, Kanagawa, Japan; ^dBiostatistics Center, Massachusetts General Hospital, Harvard Medical School, Boston, Massachusetts, USA; ^eKnight Cardiovascular Institute, Oregon Health and Science University, Portland, Oregon, USA; and the ^fDivision of Cardiology, Kyung Hee University Hospital, Seoul, South Korea. *Drs Kinoshita and Suzuki contributed equally to this work.

The authors attest they are in compliance with human studies committees and animal welfare regulations of the authors' institutions and Food and Drug Administration guidelines, including patient consent where appropriate. For more information, visit the [Author Center](#).

Manuscript received May 2, 2023; revised manuscript received August 8, 2023, accepted August 10, 2023.

Optical coherence tomography (OCT) is a high-resolution imaging modality (10–15 μm) that can be used to evaluate coronary plaques, including features of vulnerability in vivo.^{1,2} Patients with OCT-defined vulnerable plaques have been reported to have a higher incidence of adverse clinical outcomes.^{3–8} However, OCT requires coronary catheterization, an invasive procedure, and thus cannot be used as a screening tool.

Coronary computed tomography angiography (CTA) has been increasingly used in clinical practice in recent years. CTA provides noninvasive assessments of coronary atherosclerosis, including plaque burden, morphology, and vascular inflammation, which may lead to tailored therapy and better clinical outcomes in patients with suspected coronary artery disease.^{9–11} CTA detects high-risk plaque (HRP) features including positive remodeling (PR), low-attenuation plaque (LAP), napkin-ring sign (NRS), and spotty calcification (SC).^{12–14} Although studies have demonstrated that subjects with HRP were associated with an increased risk of future cardiovascular (CV) events,^{12,13} few studies have addressed the direct association between an individual plaque and future risk. Furthermore, studies showed that absolute differences in event rates between those with and without HRP were small.^{13,15} Thus far, systematic validation of individual HRP features on CTA against high-resolution imaging modalities has not been reported.

Although several studies showed the presence of thin-cap fibroatheroma (TCFA) within HRP on CTA,^{14,16–18} the correlation with detailed plaque morphology has not been reported. In the present study, we evaluated detailed plaque characteristics according to OCT within each HRP feature on CTA in a large imaging dataset of subjects who underwent both OCT and CTA.

METHODS

STUDY POPULATION. This is an observational, single-center cohort study with prospective clinical follow-up. The Massachusetts General Hospital and Tsuchiura Kyodo General Hospital Coronary Imaging Collaboration (NCT04523194) is a recently established database in which all patients underwent both CTA and OCT before percutaneous coronary intervention (PCI). This multimodality imaging database provides the opportunity to study CTA characteristics of various pathologies with OCT as the criterion standard. Patients who presented with acute coronary syndrome (ACS) (unstable angina pectoris [UAP] or non-ST-segment elevation myocardial infarction

[NSTEMI]) or chronic coronary syndrome (CCS) from January 2011 to July 2020 were included in this study. ST-segment elevation myocardial infarction patients were not included in this study. The diagnoses of UAP, NSTEMI, and CCS are described in the [Supplemental Methods](#). All demographic and clinical data were collected at Tsuchiura Kyodo General Hospital (Ibaraki, Japan) and sent to Massachusetts General Hospital (Boston, Massachusetts, USA). The study period was chosen so that CTA image acquisition was performed using a single CT system. All CTA and OCT images were acquired at Tsuchiura Kyodo General Hospital and submitted to Massachusetts General Hospital for analysis.

From January 2011 to July 2020, 517 patients underwent CTA and OCT imaging. Of those, 11 patients whose OCT imaging was performed more than 180 days from the time of CTA,⁴ 6 patients with a history of coronary artery bypass graft surgery, 28 patients with a history of stent implantation in the culprit vessel, 12 patients with poor CTA quality, 2 patients with vasospastic angina, and 1 patient with spontaneous coronary artery dissection were excluded.

The site investigators who performed the procedure identified the culprit vessel based on clinical and angiographic information and/or left ventricular regional wall motion abnormality. When the culprit vessel was not obvious in the case of multivessel disease, it was chosen based on the tightest lesion in patients with CCS and the lesion with evidence of recent plaque disruption in those who presented with ACS. Of note, all of these lesions were confirmed by OCT. All coronary segments of the culprit vessel >2 mm in diameter were evaluated for the presence of plaque (calcified, noncalcified, or partially calcified) on CTA.¹³ A total of 1,492 lesions were identified in 457 culprit vessels. Of those, 405 lesions that were not imaged by OCT and 12 lesions with suboptimal OCT images were excluded. Ultimately, 1,075 lesions in 448 patients were included in the analysis ([Supplemental Figure 1](#)). Written informed consent was provided by all participants for the Tsuchiura Kyodo General Hospital's institutional database for potential future investigations. Thus, a waiver of consent for the present project was granted by the Tsuchiura Kyodo General Hospital Ethics Committee.

CTA PROCEDURE. Computed tomographic (CT) image acquisition was performed with the use of a 320-slice CT scanner (Aquilion ONE, Canon Medical

ABBREVIATIONS AND ACRONYMS

ACS	= acute coronary syndrome
CTA	= coronary computed tomography angiography
CV	= cardiovascular
HRP	= high-risk plaque
LAP	= low-attenuation plaque
NRS	= napkin-ring sign
OCT	= optical coherence tomography
PCI	= percutaneous coronary intervention
PR	= positive remodeling
SC	= spotty calcification
TCFA	= thin-cap fibroatheroma
TVNLR	= target vessel nontarget lesion revascularization

Systems Corporation) in accordance with the Society of Cardiovascular Computed Tomography guidelines.¹⁹ Oral and/or intravenous beta-blockers were administered if a patient's resting heart rate was >65 beats/min. Sublingual nitroglycerin (0.3 or 0.6 mg) was administered immediately before CTA scanning. CTA images were acquired with the following protocol: tube voltage of 120 kVp, tube current from 50 to 750 mA, gantry rotation speed of 350 ms per rotation, field matrix of 512 × 512, and scan slice thickness of 0.5 mm. Acquisition of CT data and the electrocardiographic (ECG) trace were automatically started as soon as the signal density level in the ascending aorta reached a predefined threshold of 150 HU. Images were acquired after a bolus injection of 30-60 mL of contrast media (iopamidol, 370 mg iodine/mL, Bayer Yakuhin) at a rate of 3-6 mL/s, with the use of prospective ECG triggering or retrospective ECG gating with automatic tube current modulation. All scans were performed during a single breath-hold. Images were reconstructed at a window centered at 75% of the R-R interval to coincide with left ventricular diastasis.

CTA ANALYSIS. Two readers performed CTA analysis blinded to the patient's information and OCT findings. The analysis was overseen by a level-3 CTA expert (M.F.). HRP was defined as a lesion with at least 2 HRP features. The definition of each HRP feature is described in the [Supplemental Methods](#). The intra- and interobserver kappa coefficient indices were, respectively, 0.76 and 0.73 for PR, 0.80 and 0.72 for LAP, 0.78 and 0.72 for NRS, and 0.75 and 0.70 for SC. Lesions requiring stent implantation were determined by the site operator.

OCT ANALYSIS. OCT examination was performed using either a frequency-domain (C7/C8, OCT Intravascular Imaging System; St Jude Medical) or a time-domain (M2/M3 Cardiology Imaging Systems, Light-Lab Imaging) OCT system. All OCT images were analyzed at Massachusetts General Hospital by 2 independent investigators blinded to patients' data with the use of an offline review workstation (St Jude Medical). Any discordance was resolved by consensus with a third reviewer. Readers were given angiographic images with each lesion's exact location recorded, and they used anatomic landmarks (branches and ostia) to evaluate the same lesion detected by CTA.²⁰ The definitions and analysis of OCT features are described in [Supplemental Methods](#).

CLINICAL FOLLOW-UP. Clinical follow-up by telephone call or clinic visit was performed annually for up to 3 years after discharge. Ischemia-driven revascularization, cardiac death, and all-cause death were

TABLE 1 Baseline Characteristics (N = 448)

Age, y	67 (59-74)
Male	357 (79.7)
Body mass index, kg/m ²	24.7 (22.5-26.6)
Clinical presentation	
CCS	245 (54.7)
UAP	48 (10.7)
NSTEMI	155 (34.6)
Risk factors	
Hypertension	265 (59.2)
Hyperlipidemia	259 (57.8)
Diabetes mellitus	182 (40.6)
Chronic kidney disease	131 (29.2)
Current smoker	131 (29.2)
Previous PCI	78 (17.4)
History of MI	59 (13.2)
Laboratory data	
LDL-C, mg/dL	103 (83-129)
HDL-C, mg/dL	46 (40-56)
Triglyceride, mg/dL	123 (85-182)
HbA _{1c} , %	5.9 (5.6-6.6)
eGFR, mL/min/1.73 m ²	72 (62-83)
Time from coronary CTA to OCT, d	8 (0-40)
Medication before PCI	
P2Y12 inhibitor	144 (32.1)
Aspirin	181 (40.4)
ARB/ACE inhibitor	276 (61.6)
Beta-blocker	159 (35.5)
Statin	227 (50.7)

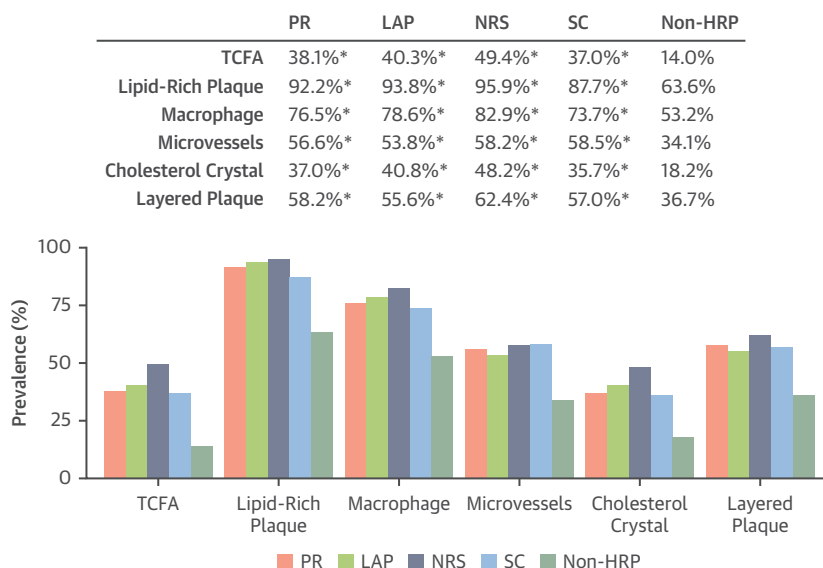
Values are median (IQR), n (%), or mean ± SD.

ACE = angiotensin-converting enzyme; ARB = angiotensin II receptor blocker; CCS = chronic coronary syndrome; CTA = computed tomography angiography; eGFR = estimated glomerular filtration rate; HbA_{1c} = glycosylated hemoglobin; HDL-C = high-density lipoprotein cholesterol; LDL-C = low-density lipoprotein cholesterol; MI = myocardial infarction; NSTEMI = non-ST-segment elevation myocardial infarction; OCT = optical coherence tomography; PCI = percutaneous coronary intervention; UAP = unstable angina pectoris.

recorded. Ischemia-driven revascularization was defined as repeated PCI or coronary artery bypass grafting of the lesion, which was determined by scintigram, physiology test (eg, fractional flow reserve), or the combination of typical angina and severe angiographic stenosis. The target lesion was defined as the treated segment including the 5-mm margin proximal and distal to the stent. Target vessel nontarget lesion revascularization (TVNLR) was defined as ischemia-driven revascularization of the target vessel for pre-existing disease, disease progression, or other reasons unrelated to the target lesion, following the ARC-2 consensus.²¹ Death was classified as cardiac unless a definite noncardiac cause was present. Each patient was classified as having untreated HRP if HRP was present at a site where PCI had not been performed.

STATISTICAL ANALYSIS. Continuous variables with normal distribution were expressed as mean ± SD,

FIGURE 1 Prevalence of OCT Features of Plaque Vulnerability Among Each HRP Feature



Compared with non-high risk plaque (HRP), optical coherence tomography (OCT)-defined vulnerable features were more prevalent in lesions containing any coronary computed tomography angiography (CTA)-defined HRP features ($P < 0.001$ for all). TCFA identified by OCT was 3 times more prevalent in HRP features than in non-HRP. Lipid-rich plaque, macrophage, microvessels, cholesterol crystals, and layered plaques were 1.4-2.6 times more frequent in HRP features. LAP = low-attenuation plaque; NRS = napkin-ring sign; PR = positive remodeling; SC = spotty calcification; TCFA = thin-cap fibroatheroma. * $P < 0.001$ vs non-HRP.

whereas median (IQR) was used for nonnormally distributed variables. In comparing patient baseline characteristics, normally distributed variables were compared with the use of Student's *t*-test, whereas nonnormally distributed variables were compared with the use of the Mann-Whitney *U*-test. Categorical data were expressed as absolute frequencies and percentages and compared with the use of the chi-square test or Fisher test, as appropriate. The normality of distribution was evaluated by means of the Kolmogorov-Smirnov test. In OCT analysis of lesions, comparisons between different groups were performed using a generalized estimating equations (GEE) approach with logit link (for binary dependent variables) or identity link (for continuous dependent variables) under the independent working correlation structure to take into account the potential clustering of multiple lesions in a single patient.²² Wald's chi-square post hoc test was conducted after fitting the between-group comparison model using GEE. Tukey's honestly significant difference test was used for multiple comparisons. Univariable and multivariable GEE log-binomial regression models were used to identify the impact of individual HRP features on identifying OCT features. Variables with *P* values < 0.10 in the univariable test were entered into the multivariable modeling. Multiplicative

interaction terms were used to test for effect modification of clinical presentation (CCS or ACS) on the association between each HRP feature and OCT feature of vulnerability. The cumulative incidence function was used to estimate the cumulative incidence rates of TVNLR and the composite outcome of TVNLR and cardiac death, taking into account competing risks with all-cause death. The comparison of cumulative incidence rates between patients with untreated HRP and those without was performed by Gray's test. A 2-sided value of $P < 0.05$ was considered to be statistically significant. Statistical analyses were performed with the use of R version 4.0.2 (R Foundation for Statistical Computing).

RESULTS

BASILINE CHARACTERISTICS. A total of 448 patients were included in this study. Baseline characteristics are summarized in Table 1. The median age was 67 years, and 79.7% were male. One-half of the patients presented with ACS. The median time interval between CTA and OCT imaging was 8 days (IQR: 0-40 days).

CTA-DETECTED LESION CHARACTERISTICS. The lesions were divided into 3 groups according to the number of HRP features present ($\text{HRP} \geq 2$,

TABLE 2 Generalized Estimating Equation Log-Binomial Regression of Each Optical Coherence Tomography Feature

	Univariable		Multivariable	
	OR (95% CI)	P Value	OR (95% CI)	P Value
Thin-cap fibroatheroma				
PR	3.23 (2.38-4.38)	<0.001	2.14 (1.47-3.10)	<0.001 ^a
LAP	2.56 (1.94-3.36)	<0.001	1.41 (1.00-1.99)	0.049 ^a
NRS	2.94 (2.10-4.09)	<0.001	1.70 (1.18-2.45)	0.005 ^a
SC	1.88 (1.44-2.46)	<0.001	1.43 (1.07-1.91)	0.015 ^a
Lipid-rich plaque				
PR	5.76 (4.11-8.07)	<0.001	3.20 (2.17-4.73)	<0.001 ^a
LAP	5.57 (3.71-8.35)	<0.001	2.37 (1.49-3.76)	<0.001 ^a
NRS	6.19 (2.88-13.30)	<0.001	1.93 (0.87-4.31)	0.108
SC	2.02 (1.43-2.85)	<0.001	1.34 (0.92-1.97)	0.126
Macrophage				
PR	2.46 (1.89-3.21)	<0.001	1.75 (1.28-2.38)	<0.001 ^a
LAP	2.33 (1.76-3.09)	<0.001	1.48 (1.08-2.04)	0.016 ^a
NRS	2.56 (1.64-3.98)	<0.001	1.52 (0.94-2.45)	0.085
SC	1.51 (1.13-2.02)	0.005	1.20 (0.88-1.63)	0.253
Microvessels				
PR	2.07 (1.63-2.64)	<0.001	2.01 (1.47-2.74)	<0.001 ^a
LAP	1.37 (1.07-1.76)	0.012	0.84 (0.60-1.18)	0.312
NRS	1.55 (1.12-2.14)	0.008	1.11 (0.76-1.62)	0.599
SC	1.86 (1.42-2.40)	<0.001	1.59 (1.21-2.10)	0.001 ^a
Cholesterol crystal				
PR	2.45 (1.82-3.30)	<0.001	1.54 (1.07-2.20)	0.020 ^a
LAP	2.46 (1.85-3.27)	<0.001	1.64 (1.15-2.33)	0.006 ^a
NRS	2.64 (1.89-3.69)	<0.001	1.64 (1.12-2.41)	0.012 ^a
SC	1.61 (1.23-2.10)	0.001	1.28 (0.96-1.69)	0.093
Layered plaque				
PR	2.11 (1.63-2.74)	<0.001	2.06 (1.50-2.83)	<0.001 ^a
LAP	1.41 (1.10-1.81)	0.007	0.84 (0.61-1.15)	0.274
NRS	1.77 (1.26-2.50)	0.001	1.33 (0.91-1.94)	0.142
SC	1.53 (1.18-1.97)	0.001	1.28 (0.98-1.67)	0.072

All high-risk plaque features were included in univariable generalized estimating equation log-binomial regression analysis to identify each optical coherence tomography feature of plaque vulnerability. Variables values of $P < 0.10$ in the univariable test were entered into the multivariable modeling. ^a $P < 0.05$ in the multivariable analysis.

LAP = low-attenuation plaque; NRS = napkin-ring sign; PR = positive remodeling; SC = spotty calcification.

HRP = 1, and non-HRP). The specific HRP features present in each group are summarized in [Supplemental Table 1](#). Among 1,075 plaques, 527 (49%) had at least 2 HRP features, 240 (22%) had 1 feature of HRP, and 308 (29%) were non-HRP. In the entire group, PR was the most prevalent feature, followed by LAP, SC, and NRS (58.1%, 40.8%, 38.5%, and 15.8%, respectively). PR and SC were dominant, and LAP and NRS were uncommon in HRP = 1 (45.4%, 42.5%, 10.8%, and 1.2%, respectively), whereas LAP and NRS increased 7- and 26-fold in frequency, respectively, in HRP ≥ 2 . A Venn diagram showed that LAP and NRS were rarely observed within lesions without PR ([Supplemental Figure 2](#)).

THE PREVALENCE OF OCT FEATURES OF VULNERABILITY IN LESIONS WITH HRP FEATURES.

The prevalence of OCT features of plaque vulnerability was similar among the 4 CTA-defined HRP features ([Figure 1](#)). Compared with non-HRP, OCT-defined vulnerable features were more prevalent in lesions containing any HRP feature ($P < 0.001$ for all). The prevalence of TCFA was 2.6-3.5 times higher in each HRP feature compared with non-HRP (37.0%-49.4% vs 14.0%). All 4 HRP features had a high prevalence of lipid-rich plaque and macrophage (87.7%-95.9% and 73.7%-82.9%, respectively). Microvessels, cholesterol crystals, and layered plaques were 1.5-2.6 times more frequent in each HRP feature than in non-HRP (53.8%-58.5% vs 34.1%, 35.7%-48.2% vs 18.2%, and 55.6%-62.4% vs 36.7%, respectively). These relationships were consistent after excluding 33 patients with the time-domain OCT system ([Supplemental Figure 3](#)) and in culprit lesions of patients who presented with ACS or CCS ([Supplemental Figures 4 and 5](#)). There was no interaction between each HRP feature and clinical presentation (ACS or CCS) for identifying each OCT feature of vulnerability in culprit lesions ([Supplemental Table 2](#)). Calcified plaques were rarely observed as an underlying pathology for ACS among culprit lesions with any HRP feature ([Supplemental Figure 6](#)). PR showed the highest negative predictive value of all OCT features of vulnerability ([Supplemental Figure 7](#)).

MULTIVARIABLE ANALYSIS FOR IDENTIFYING OCT FEATURES OF PLAQUE VULNERABILITY.

Multivariable analyses to evaluate individual associations between each HRP feature and each OCT feature of vulnerability were conducted ([Table 2](#)). All 4 HRP features were significantly associated with TCFA. PR and LAP were associated with lipid-rich plaque and macrophage. PR and SC were associated with microvessels. PR, LAP, and NRS were associated with cholesterol crystals. Only PR was associated with layered plaque. These associations were consistent when excluding 33 time-domain OCT system cases ([Supplemental Table 3](#)). The positive predictive values of the various combination patterns of HRP features for identifying TCFA are shown in [Supplemental Figure 8](#).

THE NUMBER OF HRP FEATURES AND OCT CHARACTERISTICS.

The prevalence of TCFA, lipid-rich plaque, and macrophage was significantly higher in HRP ≥ 2 than in HRP = 1 and in HRP = 1 than in non-HRP (TCFA: 40.2% vs 22.9% vs 14.0%; lipid-rich plaque: 93.5% vs 78.8% vs 63.6%; macrophage: 77.4% vs 67.5% vs 53.2%) ([Figure 2](#)). Additional OCT findings are summarized in [Table 3](#). All qualitative and quantitative OCT features of vulnerability were the highest in HRP ≥ 2 .

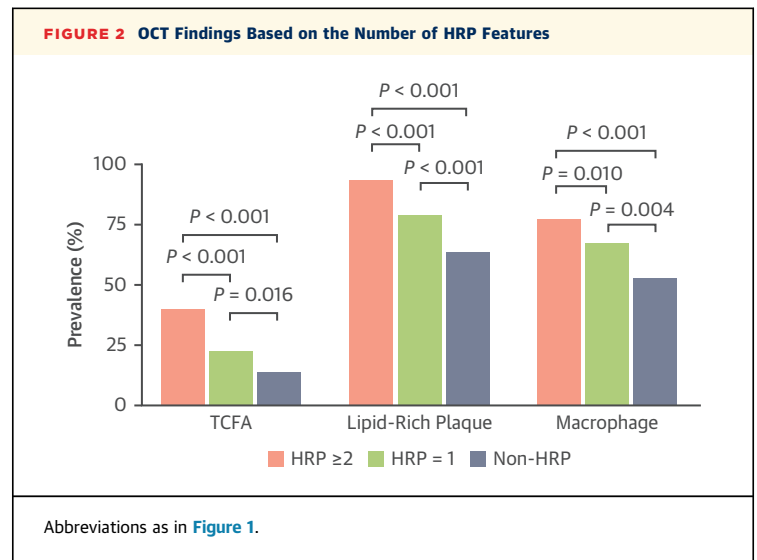
CLINICAL OUTCOME. Clinical follow-up was obtained in 445 patients (99.3%). During a median follow-up period of 31 months, 9 patients developed endpoints of TVNLR ($n = 8$, 1.8%) or cardiac death ($n = 1$, 0.2%). The comparison of clinical characteristics between patients with adverse clinical outcomes and those without showed no significant differences between the 2 groups (Supplemental Tables 4 and 5). The cumulative incidence of the composite endpoint (TVNLR and cardiac death) was significantly higher in patients with untreated HRP than in those without (4.7% vs 0.5%; $P = 0.010$) (Figure 3A, Supplemental Table 6). This difference was driven by TVNLR (4.1% vs 0.5%; $P = 0.020$) (Figure 3B).

DISCUSSION

This study demonstrated that: 1) all HRP features were associated with TCFA; 2) PR was the most prevalent feature and was associated with all OCT features of plaque vulnerability, whereas other HRP features were associated with a specific subset of OCT features of vulnerability; 3) as the number of HRP features increased, TCFA, lipid-rich plaque, and macrophage became more prevalent; and 4) untreated HRP in a culprit vessel was associated with a higher incidence of CV events.

HRP FEATURES AND PLAQUE VULNERABILITY.

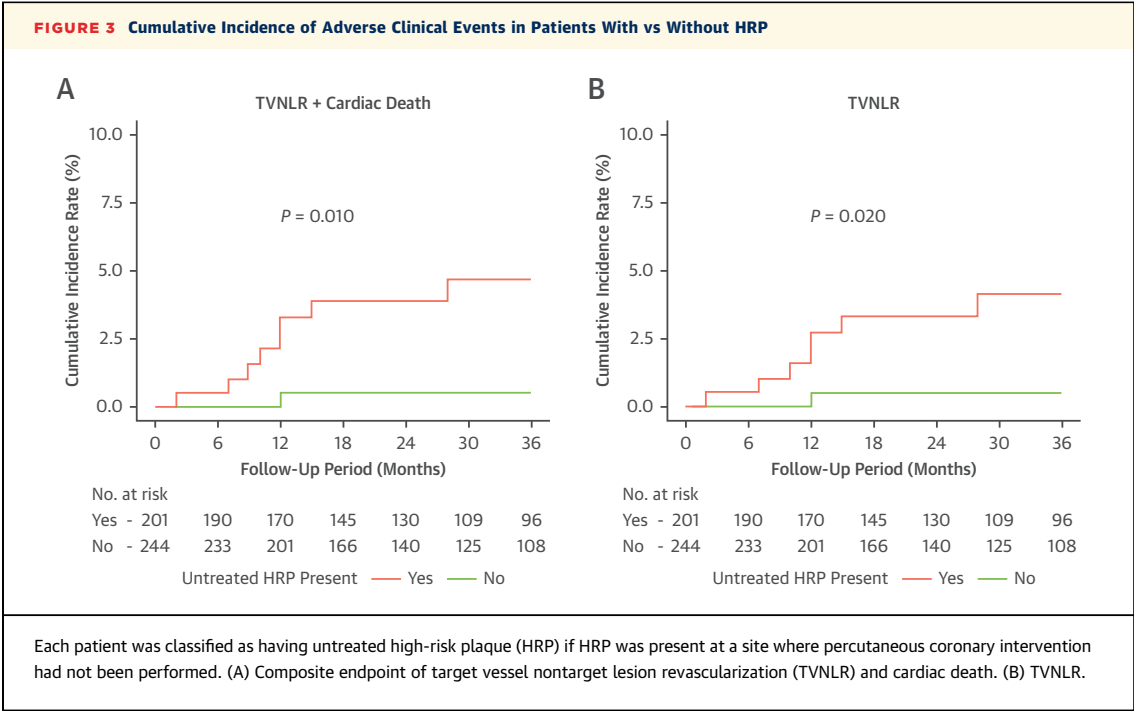
Noninvasive evaluation of rupture-prone coronary plaques has been performed primarily by means of CTA, and HRP has been considered to be a CTA equivalent of vulnerable plaque.^{14,16,23-25} Several studies reported the correlation between HRP and OCT features of plaque vulnerability.^{16-18,23,24} Most



studies enrolled only lesions with significant stenosis and consistently demonstrated that NRS was associated with TCFA. Only 1 study included nonstenotic lesions, demonstrating that low attenuation area and concomitant calcification could identify TCFA.²⁴ In contrast, the association between PR and TCFA was inconsistent in those studies,^{16-18,23,24} despite PR being considered the most related to the increased risk for future CV events.^{12,26} Thus, the correlations between individual HRP features and OCT features of plaque vulnerability are scarce, especially for features other than TCFA. Furthermore, the definition of HRP has varied among studies^{12,13,15} and HRP features on CTA have not been systematically validated against a

TABLE 3 Optical Coherence Tomography Findings

	HRP ≥2 (n = 527)	HRP = 1 (n = 240)	Non-HRP (n = 308)	P Value	P Value for Post Hoc Analysis		
					HRP ≥2 vs HRP = 1	HRP ≥2 vs Non-HRP	HRP = 1 vs Non-HRP
Qualitative analysis							
Microvessels	294 (55.8)	129 (53.8)	105 (34.1)	<0.001	0.852	<0.001	<0.001
Cholesterol crystal	208 (39.5)	54 (22.5)	56 (18.2)	<0.001	<0.001	<0.001	0.483
Layered plaque	305 (57.9)	125 (52.1)	113 (36.7)	<0.001	0.319	<0.001	0.002
Ruptured plaque	129 (24.5)	19 (7.9)	13 (4.2)	<0.001	<0.001	<0.001	0.146
Thrombus	136 (25.8)	30 (12.5)	18 (5.8)	<0.001	<0.001	<0.001	0.021
Quantitative analysis							
Maximal lipid arc, °	236 ± 106	172 ± 105	140 ± 118	<0.001	<0.001	<0.001	0.007
Lipid index	1,289 (761-2,189)	714 (181-1,304)	345 (0-915)	<0.001	<0.001	<0.001	0.006
Macrophage grade	8 (2-16)	4 (0-10)	2 (0-7)	<0.001	<0.001	<0.001	0.073
Area stenosis, %	67 ± 21	54 ± 23	52 ± 22	<0.001	<0.001	<0.001	0.713
MLA, mm ²	2.6 ± 2.3	3.9 ± 3.0	3.7 ± 3.1	<0.001	<0.001	<0.001	0.783
Values are n (%), median (IQR), or mean ± SD HRP = high-risk plaque; MLA = minimum lumen area.							



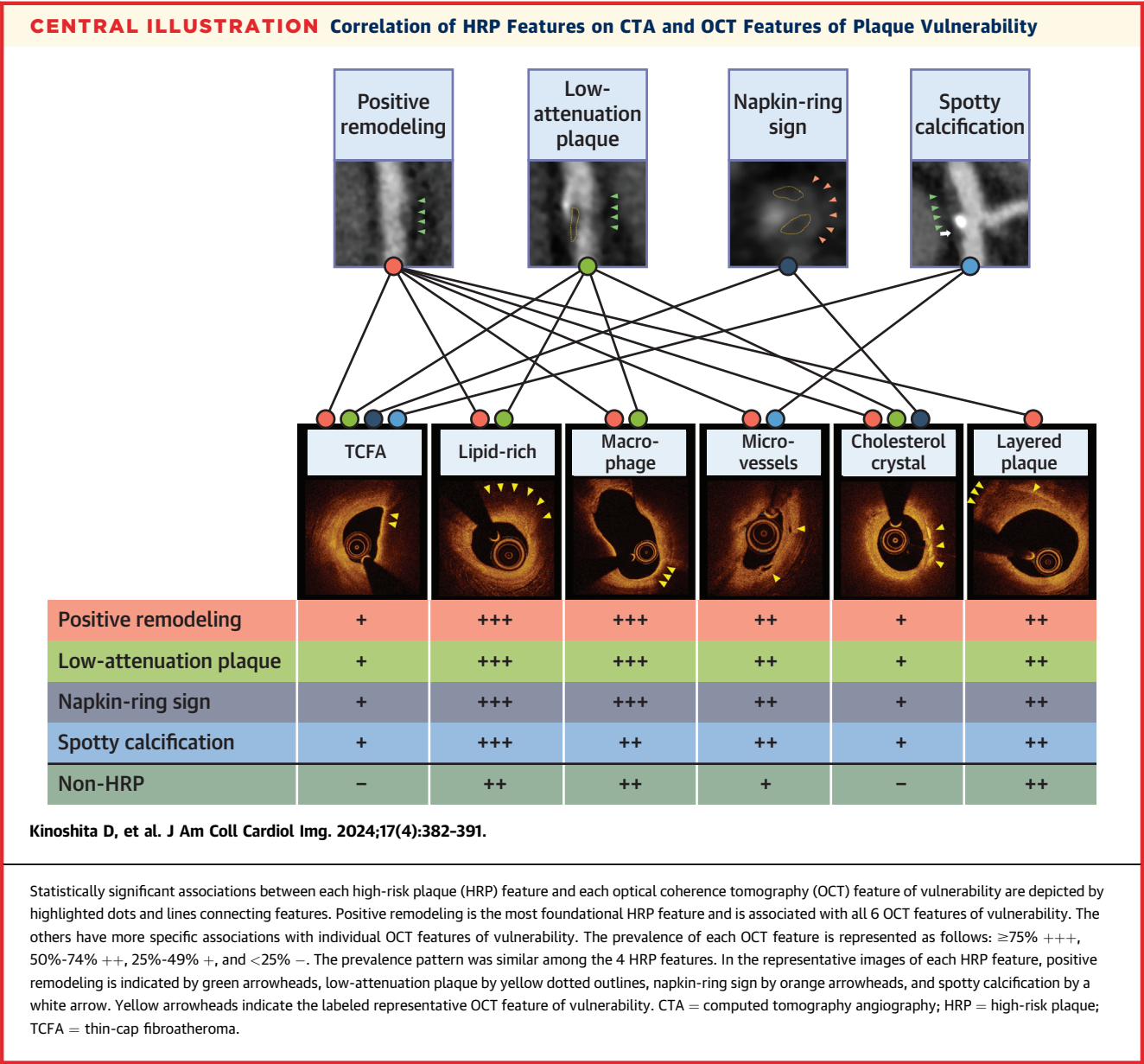
high-resolution imaging modality. In the present study, PR was the most prevalent feature and was associated with every OCT feature of plaque vulnerability. The other HRP features primarily coexisted with PR (Supplemental Figure 2), and the prevalence of OCT features of vulnerability was similar among all 4 HRP features. However, the multivariable analysis revealed that LAP, NRS, and SC had more specific relationships with particular OCT features (Central Illustration). This finding might indicate that PR is the principal consequence of chronic plaque inflammation²⁷ and that the other HRP features might reflect specific pathways leading to plaque vulnerability.

In the present study, all 4 HRP features were associated with TCFA, which is consistent with previous studies showing that all HRP features were related to necrotic core formation.^{14,16,28,29} PR and LAP were related to lipid-rich plaque and macrophage, which is in line with previous studies,^{16,28,30,31} showing that PR was associated with a larger lipid arc¹⁶ and that the region of LAP on CTA spatially correlated with lipid-rich plaque on near-infrared spectroscopy.²⁸ A higher remodeling index on CTA³² and a larger LAP volume³⁰ were reported to be associated with higher uptake of ¹⁸F-sodium fluoride, a marker of plaque vulnerability, and larger necrotic core and macrophage infiltration in histology analysis.³²

NRS was reported to be specific for the presence of both advanced plaque and TCFA in histopathology.¹⁴ Our study also demonstrated that NRS was related to cholesterol crystals. The circumferentially extensive lipid core is associated with histologically verified thin fibrous caps and numerous cholesterol crystals.³³ OCT-defined cholesterol crystal is reportedly more prevalent in an advanced atherosclerotic plaque and is associated with plaque rupture.^{34,35} Cholesterol crystals are involved in inflammasome activation, causing further inflammatory response.³⁶

Microcalcification begins in the region of excessive inflammation surrounding the necrotic core.³⁷ Consequently, microcalcification gathers into a large mass and forms SC.³⁷ Our study demonstrated the association between SC and microvessels. This finding is consistent with an earlier study showing that microvessels were more prevalent as lipid-rich plaque contained more spotty calcium.²⁹ Microvessels may provide a conduit for inflammatory cells to get into plaques, resulting in intraplaque hemorrhage with subsequent calcification.³⁸ Thus, the presence of SC may indicate the involvement of excessive inflammation caused by inflammatory cells and red blood cells that travelled into plaques through microvessels.

Plaques with only 1 HRP feature had a higher prevalence of PR and SC, and more complex plaques



with 2 or more HRP features had a higher prevalence of LAP and NRS. This finding may indicate that remodeling and calcification are the main vascular changes in the early stage of HRP development, and that LAP and NRS become more prevalent as atherosclerosis further advances with the creation of a necrotic core. The change in vascular remodeling is known as an early vascular adaptation to atherogenesis and was well described by Glagov et al.³⁹

HRP ON CTA AND CLINICAL SIGNIFICANCE. Previous studies have reported the incremental effect of HRP features for classifying the risk for CV events.^{40,41} A significant proportion of HRP features

are related to one another and coexist within the same lesions.^{25,41} Nevertheless, little evidence exists on the risk of individual lesions with HRP features.

Previous natural history studies showed that CV events might arise from vulnerable plaque, but the positive predictive values were consistently low.^{42,43} Conversely, lesions without vulnerable plaque rarely developed CV events (0.5% at 4-year follow-up).⁴³ Another study showed that the association between HRP and CV events was weak in predicting the long-term prognosis beyond 2 years.⁴⁴ It has also been reported that the cumulative number of ACS events was similar between lesions with and without HRP features during 10-year follow-up.¹⁵ Similarly, 88 of

131 (67.2%) who developed CV events did not have HRP at baseline in PROMISE (Prospective Multicenter Imaging Study for Evaluation of Chest Pain).¹³ Motoyama et al demonstrated that plaques without HRP features could evolve into HRPs, leading to ACS,¹⁵ suggesting a dynamic nature of coronary plaques. In the present study, 63.6% of lesions without HRP features on CTA had lipid-rich plaques on OCT. Although lipid volume of these plaques was much smaller than those reported in a previous study that showed an association between lipid-rich plaque and CV events,³ these lesions might develop atherosclerosis, eventually leading to CV events.

The dichotomous definition of each HRP feature lacks information on plaque burden, which is considered a strong predictor for future myocardial infarction,⁴⁵ potentially leading to a modest association with increased CV events.¹² However, our study demonstrated that HRP was equivalent to vulnerable plaque both morphologically and in the clinical significance associated with increased CV events, indicating that the detection of HRP might help to detect patients at high risk for future CV events.

STUDY LIMITATIONS. First, this was a single-center study of patients who underwent both CTA and OCT. Patients underwent CTA first. Patients without significant stenosis on CTA (eg, myocardial infarction with nonobstructive coronary arteries) might not have undergone coronary angiography and OCT. Therefore, selection bias cannot be excluded. Second, patients with ST-segment elevation myocardial infarction were not included in this analysis. Third, all patients were enrolled in Japan. It is possible that the present results may not be generalizable to other populations. Fourth, OCT was used as the in vivo criterion standard. However, some features of OCT have not yet been fully validated by histology. Finally, although the clinical event rate is similar to that of a previous study,⁴⁶ the low frequency of adverse events restricted the opportunity to conduct multivariable analysis for adjusting confounders.

CONCLUSIONS

This study revealed that all 4 HRP features on CTA correspond to features of plaque vulnerability on OCT. Plaques with multiple HRP features exhibit a higher prevalence of vulnerable OCT features. Patients with HRP had an increased incidence of future CV events.

FUNDING SUPPORT AND AUTHOR DISCLOSURES

Dr Jang's research has been supported by Mrs. Gillian Gray through the Allan Gray Fellowship Fund in Cardiology and by Mukesh and Priti Chatter through the Chatter Foundation; and Dr Jang has received educational grants from Abbott Vascular and consulting fees from Svelte Medical Systems. Dr Ferencik has received consulting fees from Siemens Healthineers, HeartFlow, and Elucid. All other authors have reported that they have no relationships relevant to the contents of this paper to disclose.

ADDRESS FOR CORRESPONDENCE: Dr Ik-Kyung Jang, Cardiology Division, Massachusetts General Hospital, Harvard Medical School, 55 Fruit Street, GRB 800, Boston, Massachusetts 02114, USA. E-mail: ijang@mgh.harvard.edu. OR Dr Tsunekazu Kakuta, Department of Cardiovascular Medicine, Tsuchiura Kyodo General Hospital, 4-1-1 Otsuno, Tsuchiura, Ibaraki 300-0028, Japan. E-mail: kaz@joy.email.ne.jp.

PERSPECTIVES

COMPETENCY IN MEDICAL KNOWLEDGE: HRP on CTA has been reported to be associated with an increased risk of future cardiovascular events. However, detailed plaque characteristics of HRP have not been systematically studied.

TRANSLATIONAL OUTLOOK: The current study demonstrated that all 4 features of HRP have more prevalent features of plaque vulnerability on OCT and patients with HRP had a higher incidence of adverse cardiac events during a 3-year follow-up period. Patients with HRP on CTA may have additional benefits from more aggressive antiatherosclerotic therapy.

REFERENCES

- Huang D, Swanson EA, Lin CP, et al. Optical coherence tomography. *Science*. 1991;254:1178-1181.
- Araki M, Park SJ, Dauerman HL, et al. Optical coherence tomography in coronary atherosclerosis assessment and intervention. *Nat Rev Cardiol*. 2022.
- Xing L, Higuma T, Wang Z, et al. Clinical significance of lipid-rich plaque detected by optical coherence tomography: a 4-year follow-up study. *J Am Coll Cardiol*. 2017;69:2502-2513.
- Araki M, Yonetsu T, Kurihara O, et al. Predictors of rapid plaque progression: an optical coherence tomography study. *J Am Coll Cardiol Img*. 2021;14:1628-1638.
- Kurihara O, Russo M, Kim HO, et al. Clinical significance of healed plaque detected by optical coherence tomography: a 2-year follow-up study. *J Thromb Thrombolysis*. 2020;50:895-902.
- Usui E, Mintz GS, Lee T, et al. Prognostic impact of healed coronary plaque in nonculprit lesions assessed by optical coherence tomography. *Atherosclerosis*. 2020;309:1-7.
- Fujiyoshi K, Minami Y, Ishida K, et al. Incidence, factors, and clinical significance of cholesterol

crystals in coronary plaque: an optical coherence tomography study. *Atherosclerosis*. 2019;283:79-84.

8. Tian J, Dauerman H, Toma C, et al. Prevalence and characteristics of TCFA and degree of coronary artery stenosis: an OCT, IVUS, and angiographic study. *J Am Coll Cardiol*. 2014;64:672-680.

9. SCOT-HEART Investigators. CT coronary angiography in patients with suspected angina due to coronary heart disease (SCOT-HEART): an open-label, parallel-group, multicentre trial. *Lancet*. 2015;385:2383-2391.

10. Williams MC, Hunter A, Shah ASV, et al. Use of coronary computed tomographic angiography to guide management of patients with coronary disease. *J Am Coll Cardiol*. 2016;67:1759-1768.

11. Oikonomou EK, Marwan M, Desai MY, et al. Noninvasive detection of coronary inflammation using computed tomography and prediction of residual cardiovascular risk (the CRISP CT study): a post hoc analysis of prospective outcome data. *Lancet*. 2018;392:929-939.

12. Williams MC, Moss AJ, Dweck M, et al. Coronary artery plaque characteristics associated with adverse outcomes in the SCOT-HEART study. *J Am Coll Cardiol*. 2019;73:291-301.

13. Ferencik M, Mayrhofer T, Bittner DO, et al. Use of high-risk coronary atherosclerotic plaque detection for risk stratification of patients with stable chest pain: a secondary analysis of the PROMISE randomized clinical trial. *JAMA Cardiol*. 2018;3:144-152.

14. Maurovich-Horvat P, Schlett CL, Alkadhi H, et al. The napkin-ring sign indicates advanced atherosclerotic lesions in coronary CT angiography. *J Am Coll Cardiol Img*. 2012;5:1243-1252.

15. Motoyama S, Ito H, Sarai M, et al. Plaque characterization by coronary computed tomography angiography and the likelihood of acute coronary events in mid-term follow-up. *J Am Coll Cardiol*. 2015;66:337-346.

16. Ito T, Terashima M, Kaneda H, et al. Comparison of in vivo assessment of vulnerable plaque by 64-slice multislice computed tomography versus optical coherence tomography. *Am J Cardiol*. 2011;107:1270-1277.

17. Nakazato R, Otake H, Konishi A, et al. Atherosclerotic plaque characterization by CT angiography for identification of high-risk coronary artery lesions: a comparison to optical coherence tomography. *Eur Heart J Cardiovasc Imaging*. 2015;16:373-379.

18. Yang DH, Kang SJ, Koo HJ, et al. Coronary CT angiography characteristics of OCT-defined thin-cap fibroatheroma: a section-to-section comparison study. *Eur Radiol*. 2018;28:833-843.

19. Erratum to "Abstracts of the 11th annual scientific meeting of the society of cardiovascular computed tomography" [J Cardiovasc Comput Tomogr 10 (3) (2016) S1-S96]. *J Cardiovasc Comput Tomogr*. 2016;10:525.

20. Hoffmann U, Moselewski F, Nieman K, et al. Noninvasive assessment of plaque morphology and composition in culprit and stable lesions in acute coronary syndrome and stable lesions in stable angina by multidetector computed

tomography. *J Am Coll Cardiol*. 2006;47:1655-1662.

21. Garcia-Garcia HM, McFadden EP, Farb A, et al. Standardized endpoint definitions for coronary intervention trials: the Academic Research Consortium-2 Consensus Document. *Circulation*. 2018;137:2635-2650.

22. Russo M, Fracassi F, Kurihara O, et al. Healed plaques in patients with stable angina pectoris. *Arterioscler Thromb Vasc Biol*. 2020;40:1587-1597.

23. Kashiwagi M, Tanaka A, Kitabata H, et al. Feasibility of noninvasive assessment of thin-cap fibroatheroma by multidetector computed tomography. *J Am Coll Cardiol Img*. 2009;2:1412-1419.

24. Soeda T, Uemura S, Morikawa Y, et al. Diagnostic accuracy of dual-source computed tomography in the characterization of coronary atherosclerotic plaques: comparison with intravascular optical coherence tomography. *Int J Cardiol*. 2011;148:313-318.

25. Schmid M, Pfleiderer T, Jang IK, et al. Relationship between degree of remodeling and CT attenuation of plaque in coronary atherosclerotic lesions: an in-vivo analysis by multi-detector computed tomography. *Atherosclerosis*. 2008;197:457-464.

26. Lee JM, Choi G, Koo BK, et al. Identification of high-risk plaques destined to cause acute coronary syndrome using coronary computed tomographic angiography and computational fluid dynamics. *J Am Coll Cardiol Img*. 2019;12:1032-1043.

27. Papadopoulou SL, Neefjes LA, Garcia-Garcia HM, et al. Natural history of coronary atherosclerosis by multislice computed tomography. *J Am Coll Cardiol Img*. 2012;5:528-537.

28. Voros S, Rinehart S, Qian Z, et al. Coronary atherosclerosis imaging by coronary CT angiography: current status, correlation with intravascular interrogation and meta-analysis. *J Am Coll Cardiol Img*. 2011;4:537-548.

29. Kataoka Y, Puri R, Hammadah M, et al. Spotty calcification and plaque vulnerability in vivo: frequency-domain optical coherence tomography analysis. *Cardiovasc Diagn Ther*. 2014;4:460-469.

30. Kwiecinski J, Dey D, Cadet S, et al. Predictors of 18F-sodium fluoride uptake in patients with stable coronary artery disease and adverse plaque features on computed tomography angiography. *Eur Heart J Cardiovasc Imaging*. 2020;21:58-66.

31. Joshi NV, Vesey AT, Williams MC, et al. 18F-fluoride positron emission tomography for identification of ruptured and high-risk coronary atherosclerotic plaques: a prospective clinical trial. *Lancet*. 2014;383:705-713.

32. Wen W, Gao M, Yun M, et al. In vivo coronary 18F-sodium fluoride activity: correlations with coronary plaque histological vulnerability and physiological environment. *J Am Coll Cardiol Img*. 2022.

33. Goldstein JA, Grines C, Fischell T, et al. Coronary embolization following balloon dilation of lipid-core plaques. *J Am Coll Cardiol Img*. 2009;2:1420-1424.

34. Katayama Y, Tanaka A, Taruya A, et al. Feasibility and clinical significance of in vivo cholesterol

crystal detection using optical coherence tomography. *Arterioscler Thromb Vasc Biol*. 2020;40:220-229.

35. Qin Z, Cao M, Xi X, et al. Cholesterol crystals in nonculprit plaques of STEMI patients: a 3-vessel OCT study. *Int J Cardiol*. 2022;364:162-168.

36. Tall AR, Westerterp M. Inflammasomes, neutrophil extracellular traps, and cholesterol. *J Lipid Res*. 2019;60:721-727.

37. Nakahara T, Dweck MR, Narula N, Pisapia D, Narula J, Strauss HW. Coronary artery calcification: from mechanism to molecular imaging. *J Am Coll Cardiol Img*. 2017;10:582-593.

38. Kolodgie FD, Gold HK, Burke AP, et al. Intraplaque hemorrhage and progression of coronary atheroma. *N Engl J Med*. 2003;349:2316-2325.

39. Glagov S, Weisenberg E, Zarins CK, Stankunavicius R, Koletts GJ. Compensatory enlargement of human atherosclerotic coronary arteries. *N Engl J Med*. 1987;316:1371-1375.

40. Motoyama S, Sarai M, Harigaya H, et al. Computed tomographic angiography characteristics of atherosclerotic plaques subsequently resulting in acute coronary syndrome. *J Am Coll Cardiol*. 2009;54:49-57.

41. Otsuka K, Fukuda S, Tanaka A, et al. Napkin-ring sign on coronary CT angiography for the prediction of acute coronary syndrome. *J Am Coll Cardiol Img*. 2013;6:448-457.

42. Stone GW, Maehara A, Lansky AJ, et al. A prospective natural-history study of coronary atherosclerosis. *N Engl J Med*. 2011;364:226-235.

43. Erlinge D, Maehara A, Ben-Yehuda O, et al. Identification of vulnerable plaques and patients by intracoronary near-infrared spectroscopy and ultrasound (PROSPECT II): a prospective natural history study. *Lancet*. 2021;397:985-995.

44. Yang S, Lee JM, Hoshino M, et al. Prognostic implications of comprehensive whole vessel plaque quantification using coronary computed tomography angiography. *J Am Coll Cardiol Asia*. 2021;1:37-48.

45. Williams MC, Kwiecinski J, Doris M, et al. Low-attenuation noncalcified plaque on coronary computed tomography angiography predicts myocardial infarction: results from the multicenter SCOT-HEART trial (Scottish Computed Tomography of the Heart). *Circulation*. 2020;141:1452-1462.

46. Parasca CA, Head SJ, Mijolevic M, et al. Incidence, characteristics, predictors, and outcomes of repeat revascularization after percutaneous coronary intervention and coronary artery bypass grafting: the SYNTAX trial at 5 years. *J Am Coll Cardiol Interv*. 2016;9:2493-2507.

KEY WORDS coronary computed tomography angiography, high-risk plaque, optical coherence tomography, vulnerable plaque

APPENDIX For an expanded Methods section as well as supplemental figures and tables, please see the online version of this paper.